WEP Warwick Evans Publishing

International Journal of Mechanical and Electrical Engineering

ISSN: 3005-9615 (Print), ISSN: 3005-7132 (Online) | Volume 2, Number 1, Year 2024
DOI: https://doi.org/10.62051/ijmee.v2n1.03
Journal homepage: https://wepub.org/index.php/IJMEE/index

VSG Frequency Regulation Strategy for Adaptive Model Predictive Control

Shida Sun *, Tongliang Liu, Yinxi Deng

School of Electrical Engineering and Automation, Henan Polytechnic University, Jiaozuo, Henan, China

* Corresponding Author: Shida Sun (Email: 1946554916@qq.com)

ABSTRACT

When the active power of a Virtual Synchronous Generator (VSG) is unbalanced, the frequency will fluctuate significantly. Based on this, this article proposes an adaptive model predictive control method. By introducing a hyperbolic tangent function to construct an adaptive moment of inertia that includes frequency change and frequency change rate to provide the inertia for the island microgrid system, and the predicted model is updated in real-time; At the same time, model predictive control is used to calculate the optimal power reference value of VSG, strengthening the power support of VSG. The results indicate that under joint control improves the frequency regulation capability of VSG units and further enhances the system frequency performance, and the frequency deviation reduces from 0.15Hz to 0.05Hz, and the frequency change rate reduces from 0.58Hz/s to 0.5Hz/s. It is proved that the proposed control strategy can effectively suppress the maximum frequency offset and maximum frequency change rate during power fluctuations.

KEYWORDS

Virtual Synchronous Generator; Adaptive Inertia Control; Model Predictive Control; Frequency Optimization Control.

1. INTRODUCTION

In recent years, with the gradual increase of installed capacity of new energy, its power generation instability has become more and more serious. In order to effectively integrate various distributed new energy sources, microgrid has received extensive attention from academia and industry [1-3]. Microgrids can operate either in grid-connected conditions or in isolated island mode. When the microgrid operates in the island mode, due to the loss of the support of the large power grid and the large number of new energy units, the inertia characteristics of the microgrid are further reduced, resulting in poor anti-interference ability, which poses a threat to safe and stable operation. In order to absorb a high proportion of new energy and improve the inertia characteristics of the microgrid, VSG control algorithm can be applied in the inverter to make it show the external characteristics of synchronous generators, obtain functions such as frequency regulation and voltage regulation, and improve the stable operation ability of the microgrid [4-5]. VSG control can provide the required inertia support for microgrid, and the key parameter moment of inertia J can be adjusted adaptively to adapt to different control requirements. Reference [6] proposed a J and D collaborative adaptive control method based on the selection principle of exponential function. The parameters can be adjusted in real time, and excessive frequency change rate and frequency offset can be suppressed, thus optimizing the dynamic response performance of the system. References [7-10] comprehensively considered the energy storage capacity and SOC constraints to set the value of moment of inertia, and

adopted fuzzy control theory to make the parameter value more flexible, thus improving the frequency response characteristics of the system. In the above VSG control strategy, the reference value of active power in the active power-frequency control can be regarded as a constant, and the adjustment ability is limited. Generally, it only participates in primary frequency modulation. When the gas turbine is mainly involved in secondary frequency modulation, the frequency deviation will be large if the new energy permeability is high, which will affect the stability of the system. Therefore, VSG Control method based on Model Predictive Control has been widely concerned by researchers. Reference [11] introduced the frequency change rate to change the weighting coefficient of adaptive model predictive control, which inhibited the large frequency fluctuation when the island switched to the grid-connected mode. References [12-13] applied fuzzy control to VSG control, utilizing fuzzy control for real-time adjustment of the rotational inertia, where J is set to the optimal value to enhance the frequency stability of the system under islanding mode, fully utilizing the regulatory capability of the swing equation. The optimal rated power of the VSG was corrected using MPC method, further strengthening the support of energy storage units for power demand. In reference [14],the rotor motion equations are discretized, taking into account the hardware constraints of the system. The optimization objective is designed using frequency deviation and output weighting values to obtain the required power increment for optimizing the frequency response of the system. Reference [15] predicted the frequency deviation using rotor angular frequency increment and torque increment, enhancing the secondary frequency regulation of VSG. In reference [16], a method was proposed to achieve secondary frequency regulation using an online adaptive model to address the challenges caused by the frequent switching of inverters and changes in network structure, leading to difficulty in solving. The method is divided into two parts: the first part involves parameter identification of the adaptive model, while the second part utilizes the obtained model for rolling optimization to perform secondary frequency control.

This paper proposes an adaptive model predictive control method. By considering the current operational state of the system, it solves an optimization model that satisfies the requirements of the microgrid. This approach provides inertia support to the microgrid while generating compensatory values for active power deficits. Based on this compensation, adjustments are made to the reference value of the VSG's active power, enhancing its secondary frequency regulation capability and reducing frequency deviations during transient processes.

2. FREQUENCY CHARACTERISTICS OF ISLANDED MICROGRIDS AND VSG CONTROL STRATEGIES

2.1. Frequency Characteristics of Microgrids in Islanded Operation

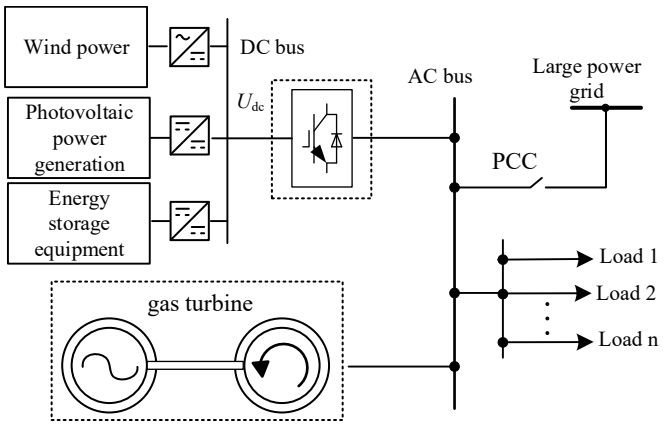

Fig 1. Simplified topology of an islanded microgrid

As shown in Fig.1, the microgrid consists of VSG operating in conjunction with renewable energy sources and energy storage, gas turbines, and loads. Unlike the main grid, microgrids lack sufficient inertia support. Therefore, when there is a sudden change in power, the frequency is prone to fluctuation, leading to significant frequency deviations and rate of change of frequency.

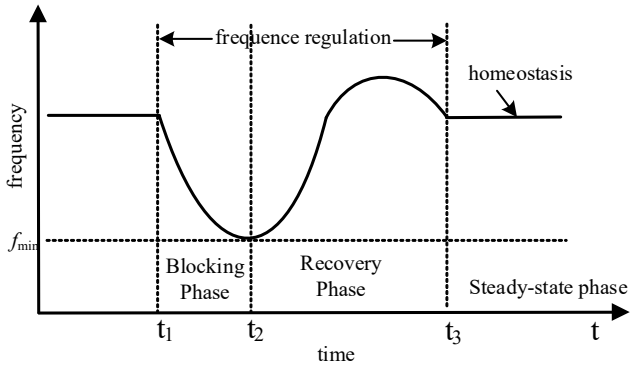

Fig 2. Frequency response process after disturbance

It can be observed from Fig.2 that when there is a disturbance in the power of the microgrid at time t_1, the frequency undergoes corresponding changes. These changes pass through three stages: blocking, recovery, and steady state. Frequency regulation includes blocking and recovery stages. In the early stages of frequency regulation, frequency control has not yet taken effect, primarily manifesting as the system's natural response. This phase involves VSG utilizing its rotor kinetic energy to inject electromagnetic power into the system, which can suppress frequency variations, but the effectiveness in offsetting frequency deviations is not ideal. During the recovery phase, the system provides continuous active power support through control strategies and corresponding frequency modulation devices, allowing the system's frequency to return to its stable value. In the steady-state phase, the frequency is maintained at a steady value.

Indicators representing system frequency include frequency deviation (including minimum frequency and steady-state minimum frequency) and frequency rate of change. When the frequency deviation exceeds the critical value, the system will disconnect the generator or shed load, causing the microgrid system to be unable to operate stably. Similarly, when the frequency rate of change exceeds the critical value, there will be instances of generator disconnection, preventing the system from increasing its output and exacerbating the system's instability, thereby preventing the frequency from returning to its steady-state value. Therefore, it is necessary to adopt different controls according to different frequency response stages to reduce the frequency rate of change and frequency deviation during frequency regulation processes, thereby achieving frequency stability in the system. Additionally, controlling the output of power sources in microgrid systems can enhance their frequency stability.

2.2. VSG Frequency Control Strategy

As shown in Fig.3, the VSG control strategy imparts inertia and damping characteristics to the power electronic inverter, suppressing sudden frequency changes.

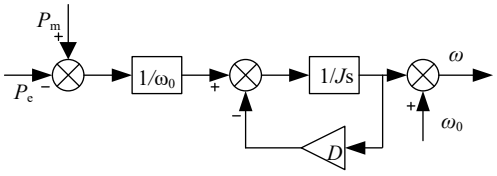

Fig 3. Block diagram of the VSG rotor equation of motion

From Fig.3, the active power-droop control equation and the rotor motion equation for VSG are expressed in equations (1) and (2) respectively.

$$P_{\mathrm{m}} = P_{\mathrm{ref}} + K_{\omega}(\omega_0 - \omega) \tag{1}$$

$$J\frac{\mathrm{d}\omega}{dt} = \frac{P_m - P_e}{\omega_0} - D\left(\omega - \omega_0\right) \tag{2}$$

Where, J is the moment of inertia, D damping coefficient, ω is the actual angular frequency, ω_0 is the rated angular frequency, P_{m} is the virtual mechanical power, P_{ref} is the VSG power instruction value, P_{e} is the VSG output power.

In the time domain, this equation can be represented as:

$$\Delta\omega = \frac{P_{\mathrm{m}} - P_{\mathrm{e}}}{D\omega_0}(1 - e^{-\frac{D}{J}t}) \tag{3}$$

From equation (3), it's evident that the rate of change of frequency depends on the damping coefficient D , the moment of inertia J , and the difference between the actual and reference active power. Therefore, during the frequency recovery phase, increasing the reference active power and raising the droop control coefficient can reduce frequency deviation. Choosing a smaller moment of inertia can shorten the time to reach steady state. On the other hand, during frequency interception, selecting a larger moment of inertia can reduce the rate of frequency change, thereby improving frequency response performance.

3. ADAPTIVE MODEL PREDICTIVE CONTROL METHOD

3.1. Design of Adaptive Controller

3.1.1. Principles of Adaptive Control

Due to the fluctuation of renewable energy output and changes in load, there is an imbalance in active power, resulting in corresponding variations in frequency and angular frequency. Fig.4 shows the curves of angular frequency and active power variations.

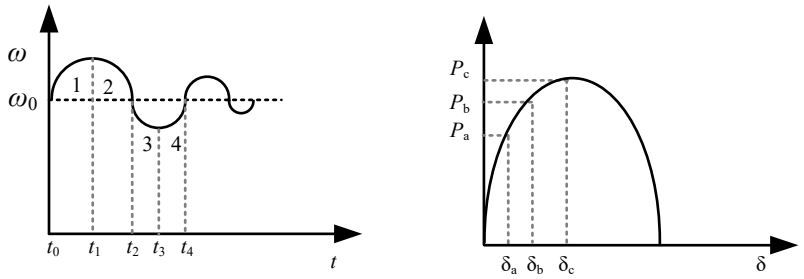

(a) Angular frequency curve (b) Power Angle curve

Fig 4. Angular frequency and power angle curves of VSG

From Fig.4, it can be seen that the system needs to go through four stages to reach a stable state from the initial state. In interval 1, $\Delta\omega$ is positive, $d\omega/dt$ is positive, requiring a larger moment of inertia to reduce the rate of frequency change; in interval 2, $\Delta\omega$ is positive, $d\omega/dt$ is negative, requiring a smaller moment of inertia to accelerate ω to ω_0; intervals 3 and 1 both require a larger moment of inertia to suppress the frequency change rate; intervals 4 and 2 both require a smaller moment of inertia to reduce the time to reach steady state. Therefore, by using the product of $\Delta\omega$ and $d\omega/dt$, taking positive and negative values respectively, different values of moment of inertia can be obtained to provide flexible support for the system's moment of inertia, adjusting the system's dynamic characteristics.

Table 1. Selection principle of J

interval	$\Delta\omega$	$d\omega/dt$	$\Delta\omega(d\omega/dt)$	J
1	positive	positive	positive	Big value
2	positive	negative	negative	Small value
3	negative	negative	positive	Big value
4	negative	positive	negative	Small value

3.1.2. Adaptive Control Design

The curve in Fig.5 depicts the relationship between rotational inertia, frequency rate of change, and frequency deviation, constructed by introducing the hyperbolic tangent function.

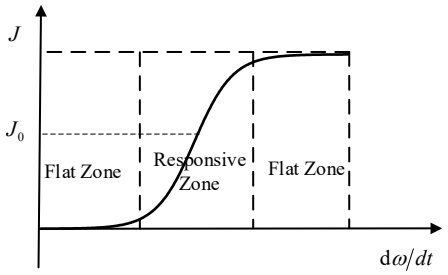

Fig 5. Hyperbolic tangent function curve

Considering the properties of monotonicity and boundedness of the hyperbolic tangent function. It can meet the requirement of the monotonic change of moment of inertia with frequency. That is, when the frequency change rate is large, a larger moment of inertia can be chosen to reduce the frequency change rate. When the frequency change rate is small, a smaller value of moment of inertia can be selected. This can rapidly change the frequency to the rated value. Meanwhile, the value of moment of inertia cannot increase infinitely due to the limitation of energy storage capacity. The hyperbolic tangent function can constrain the upper and lower limits of the moment of inertia J.

Therefore, to adapt to different operating conditions and based on the correspondence between the moment of inertia J and $\Delta\omega(d\omega/dt)$ as shown in Table.1, providing the system with variable moment of inertia, we propose an improved adaptive control strategy for moment of inertia.

$$J=\begin{cases} J_0 & |d\omega/dt|\le n \\ J_0+k\tanh(m\times|d\omega/dt|) & \Delta\omega(d\omega/dt)>0\cap|d\omega/dt|>n \\ J_0-k\tanh(m\times|d\omega/dt|) & \Delta\omega(d\omega/dt)\le 0\cap|d\omega/dt|>n \end{cases} \tag{4}$$

Where, J_0 represents the value of moment of inertia for the VSG during normal operation, where m and k are sensitivity and moment of inertia coefficients, respectively; n is the critical value of frequency change rate.

As can be seen from equation (4), the control strategy uses the positive and negative of the product of frequency deviation and frequency change rate to determine whether the system is located in the interval 1, 3 or 2, 4. When the frequency change rate is less than the critical value, J_0 is taken; when the frequency change rate exceeds the set critical value, the moment of inertia provides the corresponding value according to equation (4).

Fig.6 shows a comparison between traditional adaptive control and the adaptive control proposed in this paper. Traditional adaptive control adds a value to J_0, which can only provide a large moment of inertia to suppress the rate of frequency change. In contrast, the adaptive moment of inertia proposed in this paper can provide a large moment of inertia value when the frequency change rate is too high, and it can also provide a smaller moment of inertia during the frequency recovery phase, allowing the frequency to recover quickly.

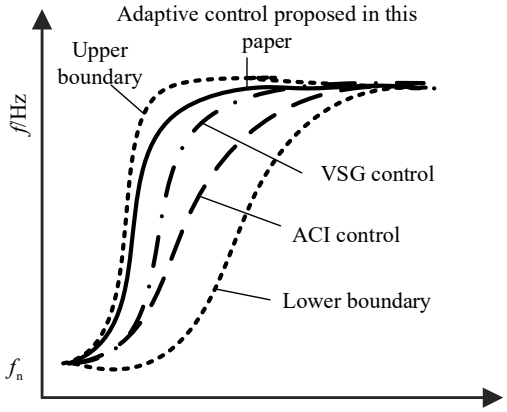

Fig 6. Moment of inertia adaptive control effect

The diagram of the adaptive moment of inertia principle is shown in Fig.7:

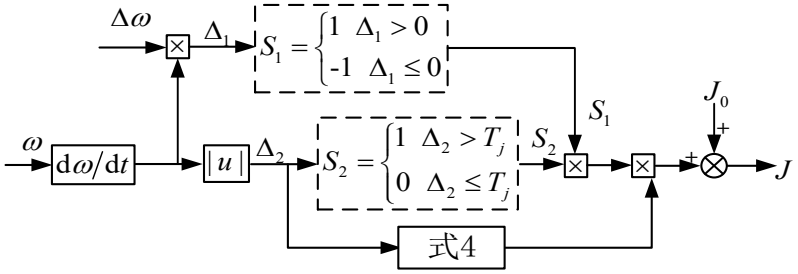

Fig 7. Schematic diagram of adaptive control of moment of inertia

3.1.3. Parameter Design

Fig.8 reflects the impact of the sensitivity coefficient m on the system, where the horizontal axis represents the angular frequency change rate, and the vertical axis represents the moment of inertia value.

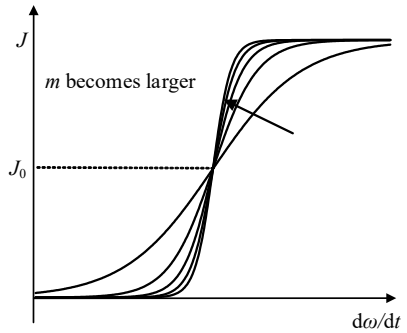

Fig 8. Hyperbolic tangent function curve when m changes

From Fig.8, it can be observed that when the value of m is relatively large, it increases the system's response speed and sensitivity, amplifying small frequency deviations. However, it may quickly enter the attenuation zone. Conversely, when m is small, the system has a larger response sensitive zone.

Therefore, it is necessary to consider both aspects when determining the value of the sensitivity coefficient *m*.

Energy storage batteries can provide moment of inertia to the system. Therefore, the magnitude of the virtual moment of inertia needs to consider both the system's output and energy storage capacity [7]. Additionally, considering the requirement for system stability, the moment of inertia value should not be too small.

$$J \le C_{\max} \frac{CU^2 - S_{\mathrm{KSOC}}}{\omega_s^2} \tag{5}$$

Where $C_{\max}$ is the maximum charge and discharge power of the energy storage battery, C is the capacitor capacitance, U is the rated voltage, and S_{ksoc} represents the energy of the energy storage SOC.

3.2. MPC Controller Design

The optimal active power output can be calculated using an MPC controller, effectively utilizing the energy storage capacity at the front end, thereby enabling the microgrid to achieve optimal active power.

3.2.1. Design of Adaptive MPC Controller

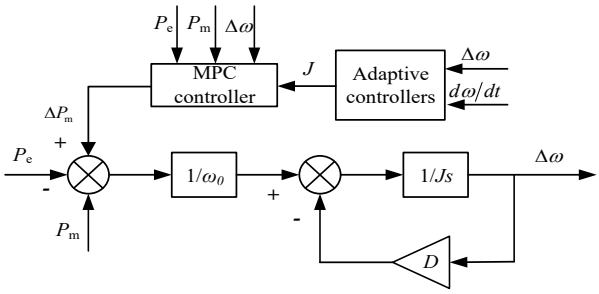

Fig 9. Adaptive MPC control structure

From Fig.9, it is evident that the MPC controller replaces the original governor. Based on the rotor motion equation, it changes the reference value of active power to alter the frequency response characteristics. When the system's frequency changes, the corresponding active power also changes, thereby predicting changes in active power to reduce system frequency fluctuations.

$$\begin{cases} \dfrac{\mathrm{d}\Delta\omega}{dt} = -\dfrac{D}{J}\Delta\omega + \dfrac{1}{J\omega_0}(\Delta P_{\mathrm{mpc}} + P_{\mathrm{m}} - P_{\mathrm{e}}) \\ y = \Delta\omega \end{cases} \tag{6}$$

Du Hamel method is used to discretize the continuous system, the sampling time of the system is T_s, and equation (6) is discretized to:

$$\begin{cases} x(k+1) = Ax(k) + B_{\mathrm{u}}u(k) + B_{\mathrm{d}}d(k) \\ y(k) = x(k) \end{cases} \tag{7}$$

$$\begin{cases} A = e^{-\frac{D}{J}T_s} \\ B_{\mathrm{u}} = \dfrac{1}{J}\displaystyle\int_0^{T_s} e^{-\frac{D}{J}\tau} d\tau \\ B_{\mathrm{d}} = -\dfrac{1}{J}\displaystyle\int_0^{T_s} e^{-\frac{D}{J}\tau} d\tau \end{cases} \tag{8}$$

Where: $x(k+1)$ is the predicted value at the time of $k+1$; x, u, and d are $\omega-\omega_0$, ΔP_{mpc}, and $\Delta P=P_m-P_e$, respectively.

Taking into account both prediction accuracy and computational complexity, this paper chooses three-step prediction for control compensation. The prediction equation can be expressed as follows:

$$Y(k+1|k) = S_m x(k) + S_n(k) + S_o d(k) \tag{9}$$

Where: $S_m = \begin{bmatrix} A \\ A^2 \\ A^3 \end{bmatrix}, S_n = \begin{bmatrix} B_u & 0 & 0 \\ AB_u & B_u & 0 \\ A^2B_u & AB_u & B_u \end{bmatrix}, S_o = \begin{bmatrix} B_d & AB_d + B_d & A^2B_d + AB_d + B_d \end{bmatrix}^T$

The objective function is to minimize the weighted sum of the squared deviations of the system's frequency deviation $\Delta\omega$ and the VSG's rated power variation ΔP_{mpc}.

$$\min_{\Delta U} J = (Y_{ref}(k) - Y(k))^T Q(Y_{ref}(k) - Y(k)) + \Delta U(k)^T R \Delta U(k) \tag{10}$$

Where $Y_{ref}=[r(k+1)\ r(k+2)\ r(k+3)]^T$, and the Q matrix and R matrix are diagonal matrices containing the weighting information of frequency deviation and power increment respectively.

Considering that the frequency fluctuations of the system will be influenced by constraint conditions, the MPC optimization equation with constraints is obtained:

$$\begin{cases} \min\limits_{\Delta U_k} J(\omega'(k),\ \Delta U_k) \\ s.t.\quad \omega(k+i+1\,|\,k) = A\omega(k+i\,|\,k) + B_u \Delta T_m(k) + B_d \Delta T_e(k) \\ \qquad \omega(k\,|\,k) = \omega(k) \\ \qquad \omega_{min}(k+i) \le \omega(k+i) \le \omega_{max}(k+i) \end{cases} \tag{11}$$

This transforms the optimization problem of MPC into a quadratic optimization problem. Solving equation (10) yields the optimal solution ΔP_{mpc} for the system.

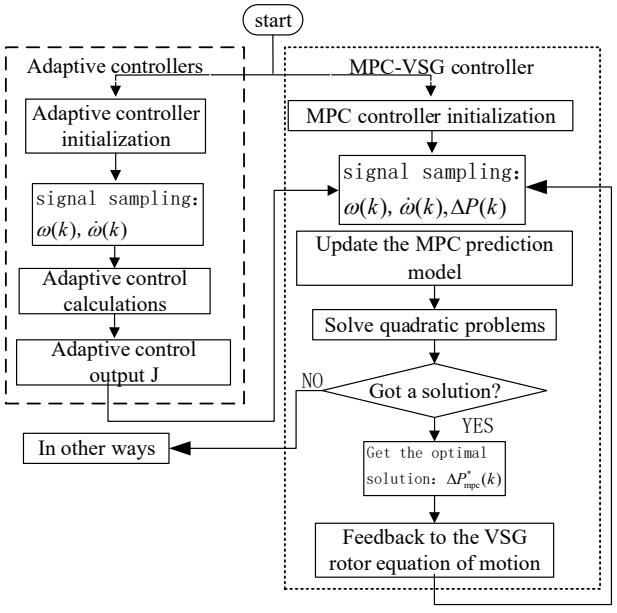

Fig 10. Adaptive MPC control flow chart

Fig.10 illustrates the control flowchart of MPC-VSG. The first step of the obtained open-loop control sequence is to apply ΔP_{mpc} to the controlled system. At the next sampling instant, the constraint optimization problem will be refreshed with new measurement values and re-solved. The first

component of the re-solved optimal value is taken, and it is inputted into the system as the control quantity.

$$\Delta U_k = [\Delta T_m(k \mid k)\ \Delta T_m(k+1 \mid k)\ ....\Delta T_m(k+p-1 \mid k)] \tag{12}$$

$$\Delta P_{\text{mpc}}(k) = [1\ 0\ 0\ 0\ 0]\Delta U \tag{13}$$

3.3. Analysis of Adaptive MPC Control

Due to the presence of constraint conditions, solving the nonlinear inequality-constrained MPC optimization problem can be divided into two cases: solutions within the feasible region and solutions outside the feasible region.

When the solution is within the feasible region, the MPC optimization problem is equivalent to the MPC optimization problem without considering constraint conditions. Define the variable γ as:

$$\gamma = \begin{bmatrix} Q(Y(k+1) - Y_{\text{ref}}(k+1)) \\ RU(k) \end{bmatrix} \tag{14}$$

The objective function is:

$$J(\Delta\omega(k),\ U(k)) = \gamma^T \gamma \tag{15}$$

Substituting the prediction equation into equation (15), we can get:

$$\gamma = \begin{bmatrix} QN \\ R \end{bmatrix} U(k) - \begin{bmatrix} QE(k+1) \\ 0 \end{bmatrix} = Aw - b \tag{16}$$

Where: $w = U(k),\ A = \begin{bmatrix} QN \\ R \end{bmatrix},\ b = \begin{bmatrix} QE(k+1) \\ 0 \end{bmatrix}$

When there is a solution to the optimization problem:

$$\frac{d\gamma^T\gamma}{dz} = 2(\frac{d\gamma}{dz})^T\gamma = 2A^T(Az-b) = 0 \tag{17}$$

Then the minimum solution can be expressed as:

$$w^* = (A^T A)^{-1} A^T b \tag{18}$$

Because $d^2(\lambda^T\gamma)/dw^2 = 2A^T A > 0$, the minimum value solution of equation (18) is the optimal solution. By combining equations (16) and (18), the optimal solution sequence of incremental power can be obtained:

$$\Delta P^*_{\text{mpc}}(k) = (S_{\text{n}}{}^T QN + R^T R)^{-1} S_{\text{n}}{}^T Q(Y_{\text{ref}} - S_{\text{m}}x(k) - S_{\text{o}}d(k)) \tag{19}$$

Let $K_{\text{mpc}}=(N^{\text{T}}QN+R^{\text{T}}R)^{-1}N^{\text{T}}Q$, then:

$$\Delta P^*_{\text{mpc}}(k) = K_{\text{mpc}} * (Y_{\text{ref}} - S_{\text{m}}x(k) - S_{\text{o}}d(k)) \tag{20}$$

Substituting equation (20) into equation (19):

$$x(k+1) = (A - B_{\text{u}}K_{\text{mpc}}S_{\text{m}})x(k) + B_{\text{u}}K_{\text{mpc}}Y_{\text{ref}} + (S_{\text{o}} - B_{\text{u}}K_{\text{mpc}}S_{\text{m}})d(k) \tag{21}$$

Considering that the eigenvalues of the matrix A-$B_{\text{u}}K_{\text{mpc}}S_{\text{m}}$ depend on T_{s}, J, D, as well as the values of the weighting coefficients q, r, adaptive control only changes the size of parameter values without

altering the model structure. Therefore, when the modulus of the eigenvalues of the matrix $A-B_uK_{mpc}S_m$ is all less than 1, the system is nominally asymptotically stable [17].

When the solution lies outside the feasible region, due to the influence of constraint conditions, the optimal solution will be constrained within the upper and lower bounds of the constraints, and the system will output power according to the values of these bounds.

4. SIMULATION VERIFICATION

In order to verify the effectiveness of the control strategy proposed in this paper, a comparison of MPC, adaptive MPC, and their frequency response characteristics under load fluctuations and fluctuations in renewable energy output is conducted. MATLAB/Simulink was used to build the model of VSG single machine with load in island mode, and the simulation parameters were shown in Table.2.

Table 2. Simulation parameters

parameter	value	parameter	value
DC bus voltage U_{dc}/V	710	Inertia J_0/kg·m^2	1.5
Grid line voltage U_n/V	380	Damping factor D_0/ω·rad/s	5
Switching frequency f_{pwm}/kHz	10	J adjustment factor k	0.5
Rated frequency f_n/Hz	50	n	0.05
Filter inductance L/mH	1.1	m	0.8
Filter capacitors C/μF	50	Power increment constraints /kW	4
Rated power /kW	6	Weight factor q	1
Sampling timeT_s/s	1e-4	Weight factor r	0.1

4.1. New Energy Output Fluctuates

In order to analyze the influence of the traditional MPC control strategy and the MPC control strategy proposed in this paper on the system when the output of new energy fluctuates, the simulation of single VSG with load in island mode is built. The simulation duration is 3.5s, The reactive power is set to 0kvar. The active power is set to 6kW, and at 0.5s, the setpoint of the active power jumps from 6kW to 9kW. At this point, adaptive rotational inertia begins to take effect. At 1.8s, the adaptive MPC kicks in to provide optimal active power compensation for the system. At 2.5s, the setpoint for active power returns to 6kW. The curves illustrating the changes in frequency and frequency rate under fluctuations in renewable energy output are shown in Fig.11 and Fig.12, respectively.

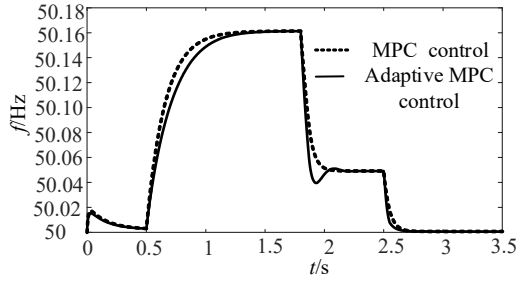

Fig 11. Output frequency curve of VSG under fluctuation of new energy output

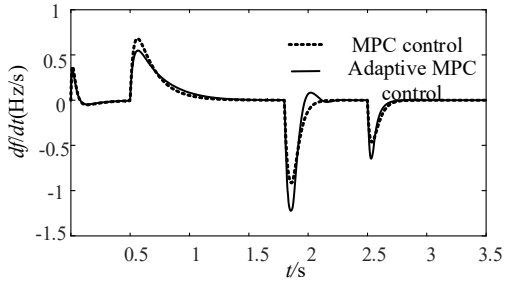

Fig 12. Frequency change rate curve of VSG under fluctuation of new energy output

It can be seen from Fig.11 that the control strategy proposed in this paper can provide a partial shortage of active power, resulting in a decrease in frequency deviation from 0.15Hz to 0.05Hz. This frequency deviation is very small, and it is approximately considered to achieve secondary frequency regulation without deviation. Additionally, it can be seen from Fig.12 that the adaptive MPC, compared to the control strategy with only MPC, reduces the frequency change rate from 0.58Hz/s to 0.5Hz/s when the output power of the new energy source fluctuates at 0.5s. This demonstrates that the control strategy proposed in this paper can reduce the rate of frequency change when fluctuations occur in new energy sources. However, due to changes in rotational inertia during the frequency recovery period, it will lead to overshoot in active power, which has no effect on steady-state conditions.

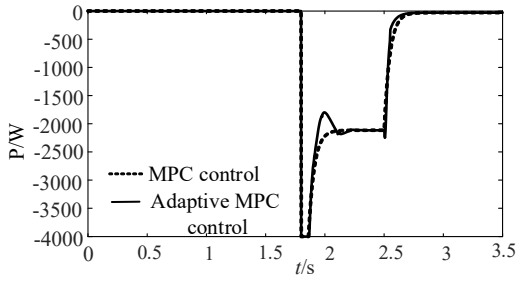

Fig 13. MPC output power increment under the fluctuation of new energy output

Fig.13 depicts the compensation power calculated by the MPC controller when the new energy output increases from 6kW to 9kW at 0.5s. As observed from the graph, at 1.8s, the MPC controller starts to take effect. Due to energy storage capacity constraints, the output is restricted to -4000W at 1.8s. With the feedback effect of power increment and constraints from the cost function, the MPC output stabilizes at -2000W. This value represents the optimal MPC compensation, achieving secondary frequency regulation.

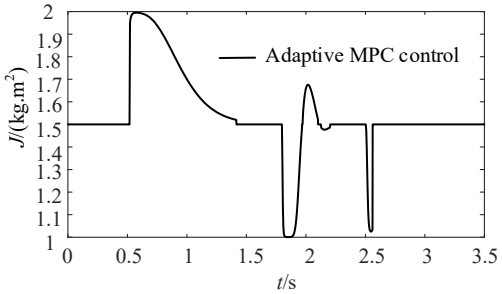

Fig 14. The value of rotational inertia *J* under the fluctuation of new energy output

Fig.14 presents the fluctuation curve of rotational inertia in the adaptive MPC control proposed in this paper. It can be observed from the graph that when the new energy output fluctuates at 0.5s, the rotational inertia takes a larger value to suppress the frequency change rate. At 1.8s, when the MPC comes into effect, it provides a smaller rotational inertia to reduce the time for the system to reach steady state. However, due to the variation in the rotational inertia, there is overshoot in active power

during the frequency recovery to steady-state values. Nevertheless, this does not affect the steady-state results. Additionally, it can be seen that at 2.5s when the active power returns to its initial value of 6kW, the rotational inertia takes a smaller value, facilitating a rapid return to steady state. Furthermore, it is evident that the proposed control strategy imposes upper and lower limits on the rotational inertia, which aligns with real-world constraints.

4.2. Load Fluctuations Occur

In order to analyze the influence of the traditional MPC control strategy and the adaptive MPC control strategy proposed in this paper on the system when the active power of the load changes, the simulation of single VSG with load in island mode is built. The simulation duration was set to 3.5s, with an initial reactive power of 0kvar given throughout the simulation. The initial active power of the load was set to 6kW. At 0.5s, the active power of the load underwent a step change from 6kW to 9kW. At this point, the adaptive rotational inertia began to take effect. At 1.8s, the adaptive MPC started to function, providing the optimal compensation for the active power to the system. At 2.5s, the active power of the load returned to 6kW. The variations in frequency and frequency change rate when the active power changes are illustrated in Fig.15 and Fig.16, respectively.

It can be seen from Fig.15 that the control strategy proposed in this paper can provide a portion of the shortfall in active power, leading to a reduction in frequency deviation from 0.15 Hz to 0.05 Hz. This small frequency deviation can be approximated to achieve secondary frequency regulation without deviation. Fig.16 indicates that compared to the control strategy with only MPC, the adaptive MPC reduces the frequency change rate from 0.58Hz/s to 0.5Hz/s when the load power changes at 0.5s. This demonstrates that the proposed control strategy can reduce the rate of frequency variation when new energy sources fluctuate. However, variations in rotational inertia during the frequency recovery period can lead to overshoot in active power, which does not affect steady-state conditions.

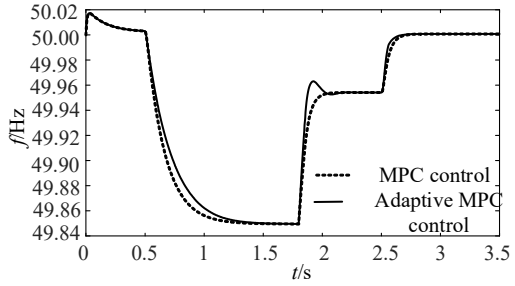

Fig 15. Output frequency curve of VSG under load throwing

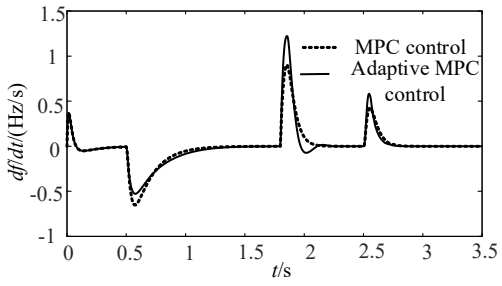

Fig 16. Output frequency change rate curve of VSG under load throwing

Fig.17 shows the compensation power calculated by the MPC controller when the load power increases from 6kW to 9kW at 0.5s. It can be seen from the figure that at 1.8s, the MPC controller begins to play a role. Due to the limitation of energy storage capacity, the output is limited to 4kW at 1.8s. The constraint of the cost function makes the MPC output stable at 2kW, which is the optimal MPC compensation and realizes the secondary frequency modulation.

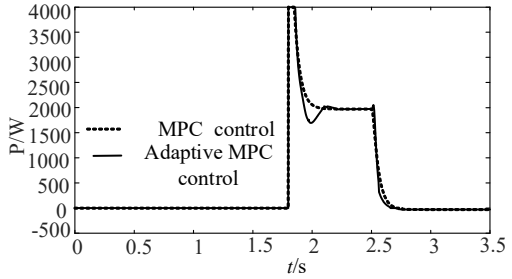

Fig 17. MPC output power increment under load throwing

Fig.18 illustrates the fluctuation curve of rotational inertia in the adaptive MPC control proposed in this paper. It can be observed from the graph that when the load fluctuates at 0.5s, the rotational inertia takes a larger value to suppress the rate of frequency variation. At 1.8s, when the MPC comes into effect, it provides a smaller rotational inertia to reduce the time for the system to reach steady state. However, due to the variation in the value of rotational inertia, there is overshoot in active power during the period of frequency recovery to the steady-state value. Nevertheless, this does not affect the steady-state results. Additionally, it can be seen that at 2.5s, when the load active power returns to its initial value of 6kW, the rotational inertia takes a smaller value, enabling a rapid return to steady state. Furthermore, it is evident from the graph that there are upper and lower constraints on the rotational inertia values in the control strategy proposed in this paper, which is consistent with practical scenarios.

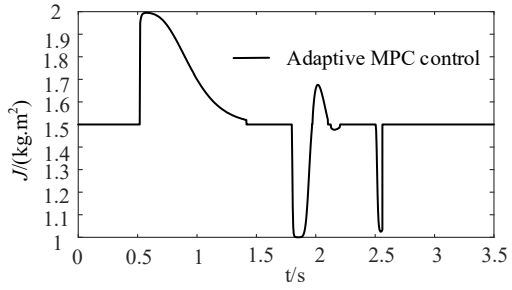

Fig 18. Value of moment of inertia J under load throwing

5. CONCLUSION

This paper focuses on the VSG as the research subject and investigates how to enhance its capability to participate in frequency regulation within microgrids. It analyzes the role of rotational inertia in the frequency regulation process and proposes a frequency modulation method that combines adaptive inertia and Model Predictive Control for VSG. This method not only improves the frequency regulation capability of VSG but also optimizes the frequency response. The following conclusions are drawn based on theoretical analysis and simulation verification:

1) An adaptive inertia control strategy is proposed. By utilizing the angular frequency deviation and angular frequency rate of change, a new rotational inertia function is constructed. Additionally, a hyperbolic tangent function is introduced, allowing the rotational inertia to flexibly adjust during frequency dynamic changes, thereby facilitating rapid frequency restoration to the rated value.

2) An adaptive model predictive control method is proposed. Based on the VSG rotation equation, the prediction model is derived, and the objective function considering the frequency fluctuation and power output limit of the system is constructed to compensate the frequency deviation caused by power imbalance in real time. This control method can improve the frequency modulation capability of VSG, the frequency deviation can be reduced from 0.15Hz to 0.05Hz, and the frequency change rate can be reduced from 0.58Hz/s to 0.5Hz/s, which is reduced by 16%, proving the correctness of adaptive model predictive control.

REFERENCES

[1] Yang Xinfa,Su Jian, Lu Zhipeng, et al. Review of Microgrid Technology[J]. Proceedings of the CSEE, 2014, 34 (01): 57-70.

[2] Kang Chongqing,Yao Liangzhong. Key scientific issues and theoretical research framework of high proportion renewable energy power system. Automation of Electric Power Systems,2017,41(09):2-11.

[3] Zheng Tianwen, Chen Laijun, Chen Tianyi, et al. Review and prospect of virtual synchronous generator technologies [J]. Automation of Electric Power Systems, 2015, 39(21):165-175.

[4] Liu Zhongjian, Zhou Ming, Li Zhaohui, et al. Review of inertia control technology and inertia demand evaluation for high proportion new energy power systems [J]. Electric Power Automation Equipment,2021,41(12):1-11+53.

[5] Yang Yun, Mei Fei, Zhang Chenyu, et al. Collaborative Adaptive Control Strategy of Moment of Inertia and Damping Coefficient of Virtual Synchronous Generator[J]. Electric Power Automation Equipment), 2019,39 (03): 125-131.

[6] Cheng Zixia, Yu Yang, Chai Xuzheng.Based on collaborative adaptive control of optical storage VSG run control research) [J]. Power system protection and control,2020,48(24):79-85.

[7] Yang Fan, Shao Yinlong, Li Dongdong, et al. Fuzzy adaptive VSG control strategy considering energy storage capacity and SOC constraints[J]. Power Grid Technology,2021,45(05):1869-1877.

[8] Li Yi, Li Yongli, Li Song, et al. Power distribution and Virtual inertia control for PV and Hybrid energy storage systems based on VSG[J]. Electric power automation equipment,2023,43(07):27-34.

[9] Torres L. M A, Lopes L A C, Moran T. L A, et al. Self-Tuning Virtual Synchronous Machine： A control strategy for energy storage systems to support dynamic frequency control[J]. IEEE Transactions on Energy Conversion, 2014, 29(4):833-840.

[10] Zhang Xing, Mao Fubin, Xu Haizhen, et al. An optimal coordination control strategy of micro-grid inverter and energy storage based on variable virtual inertia and damping of VSG[J]. Chinese Journal of Electrical Engineering, 2017, 3(3):25-33.

[11] Wang Kairang, Zhao Yiming, Meng Jianhui, et al. Smooth Grid Connection Strategy for Optical Storage Virtual Synchronous Machine Based on Adaptive Model Predictive Control [J]. High Voltage Technology,2023, 49(02): 831-839.

[12] Zhang Tao, Zheng Jiaqi, Wang Fudong, et al. VSG Moment of inertia adaptive Algorithm based on Fuzzy Control[J]. Power Electronics Technology),2021,55(01):40-44.

[13] Liao Yong. Research on Stability and Predictive Control of Permanent magnet direct drive wind-storage power generation System in isolated net[D]. Sichuan: University of Electronic Science and Technology of China, 2021.

[14] Li Shuaihu, Xiang Lizhen, Xiang Zhenyu, et al. Model predictive control method for improving VSG frequency Response [J]. High Voltage Technology, 2021, 47(08):2856-2864.

[15] Chen Laijun, Wang Ren, Zheng Tianwen, et al.. Model Predictive Control of Virtual synchronous Generator for Improving Frequency Dynamic Characteristics of independent microgrid[J]. Automation of Electric Power Systems, 2018, 42(03):40-47.

[16] Yang Xiangzhen, Yang Qiuqiang, Du Yan, et al. Secondary frequency modulation strategy of microgrid using adaptive online model identification[J]. Automation of Electric Power Systems, 2021, 45(20):121-130.

[17] Chen Hong. Model Predictive Control[M]. Beijing: Science Press, 2013.